Identification of a Heteroleptic $Pd_6L_6L'_6$ Coordination Cage by Screening of a Virtual Combinatorial Library

Sylvain Sudan,[a] Ru-Jin Li,[a] Suzanne M. Jansze,[a] André Platzek,[b] Robin Rudolf,[b] Guido H. Clever,[b] Farzaneh Fadaei-Tirani,[a] Rosario Scopelliti,[a] and Kay Severin[a]*

[a] Institut des Sciences et Ingénierie Chimiques, Ecole Polytechnique Fédérale de Lausanne (EPFL), 1015 Lausanne, Switzerland. E-mail: kay.severin@epfl.ch

[b] Fakultät für Chemie und Chemische Biologie, Technische Universität Dortmund, 44227 Dortmund, Germany

ABSTRACT: The design of structurally defined heteroleptic coordination cages is a challenging task, and only few examples are known so far. Here, we describe a selection approach, which allowed identifying a novel hexanuclear Pd cage containing two types of dipyridyl ligands. A virtual combinatorial library of $[Pd_nL_{2n}](BF_4)_{2n}$ complexes was prepared by mixing six different dipyridyl ligands with substoichiometric amounts of $[Pd(CH_3CN)_4](BF_4)_2$. Analysis of the equilibrated reaction mixture revealed the preferential formation of a heteroleptic $[Pd_6L_6L'_6](BF_4)_{12}$ assembly. The complex was prepared on preparative scale by a targeted synthesis, and its structure was elucidated by single crystal X-ray diffraction. It features an unprecedented trigonal antiprismatic cage structure, with two triangular Pd_3L_3 macrocycles bridged by six ligands L'. A related, but significantly larger $[Pd_6L_6L'_6](BF_4)_{12}$ cage was obtained by using metalloligands instead of organic dipyridyl ligands.

Palladium-based metallosupramolecular assemblies of the general formula $[Pd_nL_{2n}]X_n$ can be obtained by combination of bismonodentate N-donor ligands L with Pd(II) salts such as $Pd(NO_3)_2$ or $[Pd(CH_3CN)_4](BF_4)_2$.[1-8] Assemblies of this type display a rich structural chemistry, ranging from simple mononuclear complexes[9-12] to giant cage structures with n = 30,[13] or topologically complex interlocked structures.[14,15] Interesting host-guest chemistry was observed, and applications in the field of catalysis (nanoreactors)[16,17] and medicinal chemistry[18-24] have been explored. Furthermore, $[Pd_nL_{2n}]X_n$ complexes have been used as components of novel materials.[25-30]

Most $[Pd_nL_{2n}]X_n$ assemblies reported to date feature a single type of bridging ligand L. However, several groups have recently investigated heteroleptic complexes with two different ligands L and L'.[31-52] A key challenge in this context is the controlled formation of a particular heteroleptic complex ('integrative self-sorting'),[33] as opposed to a mixture of complexes. This challenge gets more pronounced for high numbers of n. For example, for two ligands L and L', there are six possible structures for dinuclear complexes (n = 2), and already 13 possible structures for trinuclear complexes (n = 3). It is therefore not surprising that most investigations have focused so far on the formation of heteroleptic complexes containing only two Pd^{2+} ions.[35-40] To the best of our knowledge, there are only four reports about defined heteroleptic $[Pd_nL_{2n}]X_n$ assemblies with more than two Pd^{2+} ions: a star-shaped $[Pd_5L_5L'_5](BF_4)_{10}$ complex described by Chand and co-workers,[41] a trigonal prismatic $[Pd_6L_6L'_6](NO_3)_{12}$ complex described by Mukherjee and co-workers,[42] and dodecanuclear $[Pd_{12}L_{12}L'_{12}](BF_4)_{24}$ and $[Pd_{12}L_{23}L'](NO_3)_{24}$ cages described by the group of Fujita.[43,44]

The studies on heteroleptic $[Pd_nL_{2n}]X_n$ complexes have shown that integrative self-sorting is possible by using carefully designed ligands, with special focus on steric interactions and geometric constraints. However, the rational design of defined heteroleptic complexes becomes increasingly difficult for larger assemblies. Below, we describe a selection approach, which allowed identifying a $[Pd_6L_6L'_6](BF_4)_{12}$ complex with an unprecedented trigonal antiprismatic cage structure.

A molecularly defined metallosupramolecular structure needs to have a higher thermodynamic stability than competing structures. Otherwise, rearrangement reactions would occur over time. We hypothesized that screening of a virtual combinatorial library (VCL)[53-56] of $[Pd_nL_{2n}]X_n$ complexes would allow identifying particularly stable assemblies. A VCL of Pd assemblies can be generated by using a mixture of ligands in combination with substoichiometric amounts of a Pd salt. The ligands compete for coordination to Pd^{2+}, and only highly stable assemblies will be formed. Less stable, but potentially accessible complexes will not be generated to a significant extent. We would like to note the importance of using a virtual library, as opposed to a 'real' library with stoichiometric amounts of Pd^{2+}. For the latter, the most stable assembly is not necessarily formed in larger amounts.[57,58]

For our study, we have used six dipyridyl ligands (**L1**–**L6**), the structures of which are depicted in Figure 1. All ligands have previously been employed to make homoleptic $[Pd_nL_{2n}]X_n$ assemblies. Ligand **L1** forms a tetrahedron,[47,59] **L2**–**L4** dinuclear complexes,[60-62] **L5** a dodecanuclear cage,[63] and **L6** an interlocked structure.[64] In addition, **L4** was found to promote the formation of heteroleptic $[Pd_2L_2L'_2](BF_4)_4$ complexes.[9b]

The competition experiment was performed as follows: equimolar amounts of the six ligands and $[Pd(CH_3CN)_4](BF_4)_2$ were added to a mixture of CD_3CN and CD_3NO_2 (8:2)[65] and the resulting suspension was heated for 17 h at 65 °C, resulting in the formation of a clear solution (Scheme 1). The mixture was then analyzed by ^1H NMR spectroscopy. The region between 7.4 and 9.0 ppm is crowded by ligand signals, but the signals above 9.0 ppm can be attributed to Pd-based assemblies. When comparing these signals to those of the homoleptic complexes, we found small signals corresponding to the interlocked cage $[\{Pd_2(\mathbf{L6})_4\}_2](BF_4)_8$ (SI, Figure S12). The formation of this assembly was not unexpected, given that its high stability had been noted previously.[64] In addition to the signals of $[\{Pd_2(\mathbf{L6})_4\}_2](BF_4)_8$, there were larger signals, which

could not be matched with any of the other homoleptic complexes. In order to identify the main reaction product(s), we separated the ionic $[Pd_nL_{2n}]X_n$ complexes from the remaining 'free' ligands by precipitation with Et_2O/pentane. Analysis of the ligand fraction by ^1H NMR spectroscopy showed a depletion of ligands **L1** and **L5** (SI, Figure S15). Analysis of the precipitate by ^1H NMR spectroscopy indicated the formation of one main product with high apparent symmetry. The multiplicity of the signals were in agreement with a complex containing equal amounts of **L1** and **L5**. Additional information was obtained by mass spectrometry (SI, Figure S13 and S14). Next to signals of $[\{Pd_2(\mathbf{L6})_4\}_2](BF_4)_8$, we found signals corresponding to a hexanuclear complex containing **L1** and/or **L5** (both ligand have the same mass). Taken together, the analytical data suggested that the main product of the competition experiment was an assembly of the formula $[Pd_6(\mathbf{L1})_6(\mathbf{L5})_6](BF_4)_{12}$.

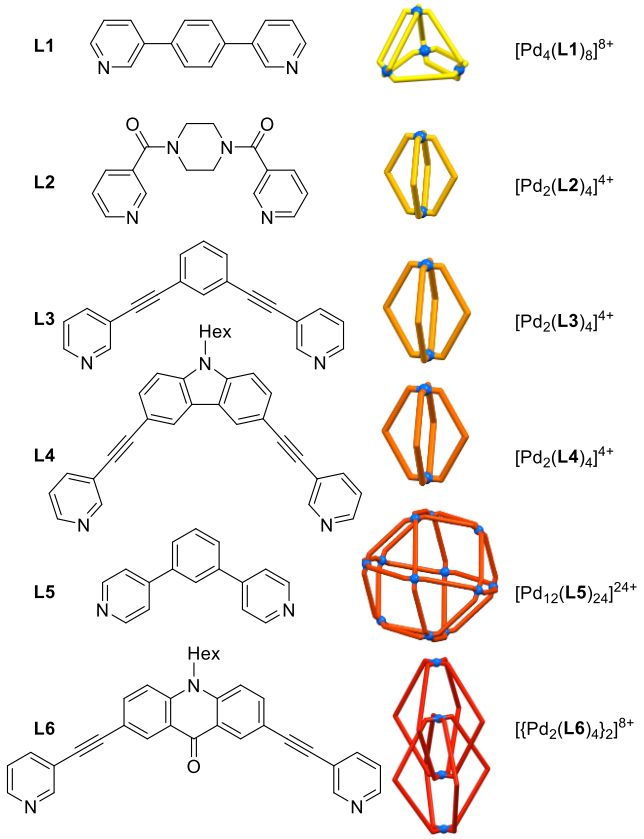

Figure 1. Structures of the N-donor ligands **L1**–**L6** and the corresponding homoleptic complexes with Pd^{2+}.

To corroborate our findings, we synthesized $[Pd_6(\mathbf{L1})_6(\mathbf{L5})_6](BF_4)_{12}$ on preparative scale by mixing equimolar amounts of **L1**, **L5**, and $[Pd(CH_3CN)_4](BF_4)_2$. The reaction product displayed the same NMR signals (SI, Figure S12), which were observed for the main product of the screening experiment. DOSY NMR spectroscopy showed that the molecular size of this new heteroleptic complex was in between that of the known homoleptic complexes $[Pd_4(\mathbf{L1})_8](BF_4)_8$ and $[Pd_{12}(\mathbf{L5})_{24}](BF_4)_{24}$ (SI, Figure S5, S10 and S22). Mass spectrometry confirmed that a hexanuclear complex had formed (SI, Figure S27 and S28).

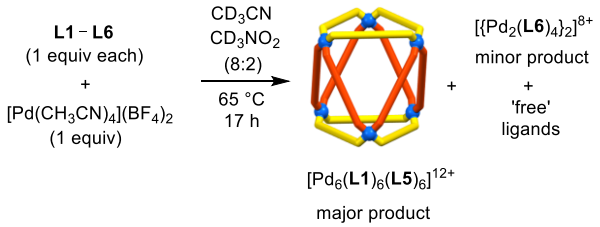

Scheme 1. The reaction of **L1**–**L6** with sub-stoichiometric amounts of Pd^{2+}.

To exclude that $[Pd_6(\mathbf{L1})_6(\mathbf{L5})_6](BF_4)_{12}$ is obtained under kinetic control, we have repeated the competition experiment with different starting conditions. Instead of using $[Pd(CH_3CN)_4](BF_4)_2$ as a source of Pd^{2+}, we have employed equimolar amounts of the preformed assemblies $[Pd_2(\mathbf{L3})_4](BF_4)_4$ and $[Pd_2(\mathbf{L4})_4](BF_4)_4$. The two complexes were equilibrated with **L1**, **L2**, **L5**, and **L6** (4 equiv each) in CD_3CN/CD_3NO_2 (Scheme 2). The ^1H NMR spectrum of the resulting mixture was very similar to what was obtained with a mixture of all six ligands (SI, Figure S16), and the heteroleptic cage $[Pd_6(\mathbf{L1})_6(\mathbf{L5})_6](BF_4)_{12}$ could be identified as the dominating Pd assembly in solution. This control experiment confirmed the superior thermodynamic stability of the heteroleptic complex.[66] We have also performed a reaction of **L1**–**L6** with stoichiometric amounts of Pd^{2+} ($[ligand]_{total}$:[Pd] = 2:1). As anticipated, the ^1H NMR spectrum of the reaction mixture was very complex (SI, Figure S18), indicating the formation of multiple assemblies instead of few selected compounds.

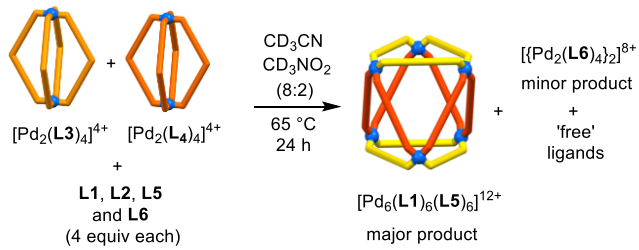

Scheme 2. Conversion of the homoleptic cages $[Pd_2(\mathbf{L3})_4](BF_4)_4$ and $[Pd_2(\mathbf{L4})_4](BF_4)_4$ into the heteroleptic cage $[Pd_6(\mathbf{L1})_6(\mathbf{L5})_6](BF_4)_{12}$.

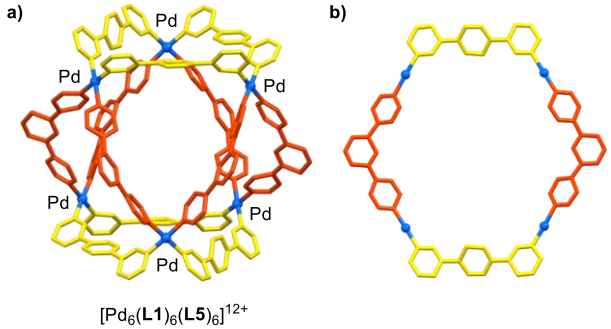

Figure 2. a) Graphic representation of the molecular structure of $[Pd_6(\mathbf{L1})_6(\mathbf{L5})_6]^{12+}$ in the crystal. b) Part of the structure showing a Pd_4 macrocyclic fragment with two ligands **L1** (yellow) and two ligands **L5** (orange). Hydrogen atoms are not depicted.

The molecular structure of $[Pd_6(\mathbf{L1})_6(\mathbf{L5})_6](BF_4)_{12}$ was analyzed by single crystal X-ray diffraction, and a graphic representation of the cationic cage is depicted in Figure 2a. The six Pd^{2+} ions occupy

the vertices of a trigonal antiprism. The two trigonal faces of the prism are composed of $[Pd_3(\mathbf{L1})_3]^{6+}$ macrocycles, which are bridged by six ligands **L5**. This highly symmetrical structure is in line with the NMR spectra, which show a single set of signals for the two ligands **L1** and **L5**.

It is interesting to note that the competition experiment with **L1**–**L6** resulted in the preferential formation of a hexanuclear complex, even though lower-nuclearity complexes are favored from an entropy point-of-view. Therefore, we assume that enthalpic effects are responsible for the high stability of $[Pd_6(\mathbf{L1})_6(\mathbf{L5})_6](BF_4)_{12}$. Inspection of the solid-state structure shows that intermolecular ligand-ligand interactions are unlikely to play a role, because the 12 ligands are well separated from each other. However, the combination of **L1** and **L5** seems to result in a particularly favorable coordination environment for the Pd^{2+} ions. The cage can be de-constructed into $[Pd_4(\mathbf{L1})_2(\mathbf{L5})_2]^{8+}$ macrocyclic fragments, one of which is shown in Figure 2b. It is evident that the geometry of the ligands allows for a 'perfect' 180 ° coordination of the metal ions. Another possible factor for the selection of **L1** and **L5** out of a pool of six ligands is the higher basicity of the aryl pyridine ligands **L1** and **L5** when compared to the alkynyl and amide-based pyridine ligands **L2**–**L4** and **L6**.[67] Finally, we have considered the possibility that anion templating effects play a role. However, the heteroleptic cage was also formed when the hexafluorophosphate complex $[Pd(CH_3CN)_4](PF_6)_2$ was combined with **L1** and **L5**, suggesting that specific anion-cage interactions are not of central importance.

Next, we have investigated if it is possible to obtain other $[Pd_6L_6L'_6]X_{12}$ assemblies of comparable topology by using ligands with a similar arrangement of the pyridyl donor atoms. The metalloligands **L7** and **L8** (Figure 3a) were used as structural analogues of the simple organic ligands **L1** and **L5**. Both ligands feature chemically inert iron clathrochelate complexes as rigid spacers between the pyridyl groups.[68] Ligand **L7** has been described before, and it forms a hexanuclear complex with Pd^{2+}.[69] The new ligand **L8** was prepared by a multi-component condensation reaction following a synthetic methodology developed in our laboratory (for details, see the SI).[70-72]

A mixture of equimolar amounts of **L7**, **L8**, and $[Pd(CH_3CN)_4](BF_4)_2$ in DMSO was heated overnight at 70 °C. Analysis of the resulting solution by ^{1}H NMR spectroscopy revealed the formation of an assembly with high apparent symmetry (single set of signals for **L7** and **L8**). The composition of this complex could be established by high resolution ESI MS. Dominant peaks for a heteroleptic assembly of the formula $\{[Pd_6(\mathbf{L7})_6(\mathbf{L8})_6](BF_4)_x\}^{z+}$ (x = 3–7; z = 9–5) could be observed (Figure 3b).

Single crystals of $[Pd_6(\mathbf{L7})_6(\mathbf{L8})_6](BF_4)_{12}$ were obtained from DMSO, but the quality of the diffraction data did not allow for a high resolution structural analysis. However, we were able to locate the Pd and Fe atoms, and their position corroborated that the complex displays a cage structure with an overall shape of a prolate spheroid. The position of the metal ions also allowed to establish the connectivity of the ligands. The six metalloligands **L7** form two $[Pd_3(\mathbf{L7})_3]^{9+}$ macrocycles, which are positioned at the opposite ends of the spheroid. The links between the two macrocycles are established by the bent metalloligands **L8**. A structural difference between the smaller cage $[Pd_6(\mathbf{L1})_6(\mathbf{L5})_6]^{12+}$ and $[Pd_6(\mathbf{L7}_6)(\mathbf{L8}_6]^{12+}$ is the connectivity of the bent ligands **L5** and **L8**. In the latter case, we observe the formation of $[Pd_2(\mathbf{L8})_2]^{4+}$ macrocycles, leading to trigonal prismatic arrangement of the six Pd^{2+} ions. We have used the crystallographic data as the basis for MMFF computations, and a model of $[Pd_6(\mathbf{L7})_6(\mathbf{L8})_6]^{12+}$ is depicted in Figure 3c.

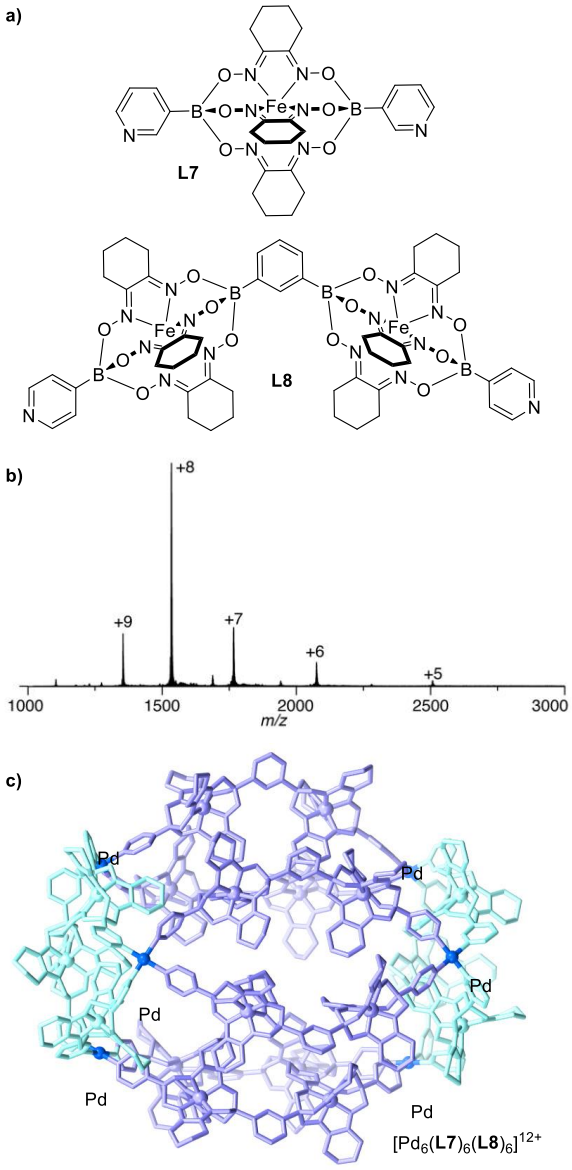

Figure 3. a) Structures of the metalloligands **L7** and **L8**. b) ESI mass spectrum of the assembly formed from **L7**, **L8**, and $[Pd(CH_3CN)_4](BF_4)_2$. c) Structure of $[Pd_6(\mathbf{L7})_6(\mathbf{L8})_6]^{12+}$ as determined by MMFF computations, with **L7** shown in cyan and **L8** shown in purple. The model is based on crystallographic data, which allowed identifying the position of the Pd and Fe atoms, and thus the connectivity of the ligands.

To summarize: we have created a virtual combinatorial library of $[Pd_nL_{2n}](BF_4)_{2n}$. complexes by mixing six different dipyridyl ligands with sub-stoichiometric amounts of $[Pd(CH_3CN)_4](BF_4)_2$. The number of potentially accessible complexes in this library is very large, but competition for a limited amount of Pd^{2+} leads to a selection process. The heteroleptic complex $[Pd_6(\mathbf{L1})_6(\mathbf{L5})_6](BF_4)_{12}$ was identified as the main Pd complex after equilibration. It is noteworthy that a *hexanuclear* complex was selected, even though none of the homoleptic complexes derived from **L1**–**L4** contain six Pd^{2+} ions (Figure 1). The preferential formation of a high-nuclearity complex with n = 6 is also remarkable, given that low-nuclearity complexes are favored from an entropy point-of-view. The results obtained with the metalloligands **L7** and **L8** demonstrate that complexes of the formula $[Pd_6L_6L'_6]X_{12}$ can be accessed with different types of dipyridyl ligands. It will be interesting to explore if other

'islands of stability' can be identified in the vast structural space of heteroleptic $[Pd_nL_{2n}]X_{2n}$. complexes.

ASSOCIATED CONTENT

Supporting Information

The Supporting Information (containing experimental details, NMR and MS spectra) is available free of charge on the ACS Publications website at DOI: XXX

AUTHOR INFORMATION

Corresponding Author

E-mail: kay.severin@epfl.ch

ORCID

Suzanne M. Jansze: 0000-0003-2979-2630
Guido H. Clever: 0000-0001-8458-3060
Farzaneh Fadaei-Tirani: 0000-0002-7515-7593
Rosario Scopelliti: 0000-0001-8161-8715
Kay Severin: 0000-0003-2224-7234

Notes

The authors declare no competing financial interests.

ACKNOWLEDGMENT

The work was supported by the Ecole Polytechnique Fédérale de Lausanne (EPFL). Funding by the Deutsche Forschungsgemeinschaft (DFG) through GRK2376 "Confinement-controlled Chemistry" - project number 331085229 and grant CL 489/2-2 is gratefully acknowledged. We thank Laura Schneider and Maike Wolters for support in ligand syntheses.

REFERENCES

(1) Saha, S.; Regeni, I.; Clever, G. H. Structure relationships between bis-monodentate ligands and coordination driven self-assemblies. *Coord. Chem. Rev.* **2018**, *374*, 1–14.
(2) Vasdev, R. A. S.; Preston, D.; Crowley, J. D. Multicavity Metallosupramolecular Architectures. *Chem. Asian J.* **2017**, *12*, 2513–2523.
(3) Clever, G. H.; Punt, P. Cation–Anion Arrangement Patterns in Self-Assembled Pd_2L_4 and Pd_4L_8 Coordination Cages. *Acc. Chem. Res.* **2017**, *50*, 2233–2243.
(4) Cook, T. R.; Stang, P. J. Recent Developments in the Preparation and Chemistry of Metallacycles and Metallacages via Coordination. *Chem. Rev.* **2015**, *115*, 7001–7045.
(5) Han, M.; Engelhard, D. M.; Clever, G. H. Self-assembled coordination cages based on banana-shaped ligands. *Chem. Soc. Rev.* **2014**, *43*, 1848–1860.
(6) Mukherjee, S.; Mukherjee, P. S. Template-free multicomponent coordination-driven self-assembly of Pd(II)/Pt(II) molecular cages. *Chem. Commun.* **2014**, *50*, 2239–2248.
(7) Harris, K.; Fujita, D.; Fujita, M. Giant hollow M_nL_{2n} spherical complexes: structure, functionalisation and applications. *Chem. Commun.* **2013**, *49*, 6703–6712.
(8) Chakrabarty, R.; Mukherjee, P. S.; Stang, P. J. Supramolecular Coordination: Self-Assembly of Finite Two- and Three-Dimensional Ensembles. *Chem. Rev.* **2011**, *111*, 6810–6918.
(9) Preston, D.; Kruger, P. E. Reversible Transformation between a $[PdL_2]^{2+}$ "Figure-of-Eight" Complex and a $[Pd_2L_2]^{4+}$ Dimer: Switching On and Off Self-Recognition. *Chem. Eur. J.* **2019**, *25*, 1781–1786.
(10) Bandi, S.; Pal, A. K.; Hanan, G. S.; Chand, D. K. Stoichiometrically Controlled Revocable Self-Assembled "Spiro" versus Quadruple-Stranded "Double-Decker" Type Coordination Cages. *Chem. Eur. J.* **2014**, *20*, 13122–13126.
(11) Sahoo, H. S.; Tripathy, D.; Chakrabortty, S.; Bhat, S.; Kumbhar, A.; Chand, D. K. Self-assembled mononuclear palladium(II) based molecular loops. *Inorg. Chim. Acta* **2013**, *400*, 42–50.
(12) Hori, A.; Yamashita, K.; Kusukawa, T.; Akasaka, A.; Biradha, K.; Fujita, M. A circular tris[2]catenane from molecular 'figure-of-eight.' *Chem. Commun*. **2004**, *16*, 1798–1799.
(13) Fujita, D.; Ueda, Y.; Sato, S.; Yokoyama, H.; Mizuno, N.; Kumasaka, T.; Fujita, M. Self-Assembly of $M_{30}L_{60}$ Icosidodecahedron. *Chem* **2016**, *1*, 91–101.
(14) Schulte, T. R.; Holstein, J. J.; Schneider, L.; Adam, A.; Haberhauer, G.; Clever, G. H. A New Mechanically-Interlocked $[Pd_2L_4]$ Cage Motif by Dimerization of two Peptide-based Lemniscates, *Angew. Chem. Int. Ed.* **2020**, *59*, 22489–22493.
(15) Frank, M.; Johnstone, M. D.; Clever, G. H. Interpenetrated Cage Structures. *Chem. Eur. J.* **2016**, *22*, 14104–14125.
(16) Jongkind, L. J.; Caumes, X.; Hartendorp, A. P. T.; Reek, J. N. H. Ligand Template Strategies for Catalyst Encapsulation. *Acc. Chem. Res.* **2018**, *51*, 2115–2128.
(17) Sinha, I.; Mukherjee, P. S. Chemical Transformations in Confined Space of Coordination Architectures. *Inorg. Chem.* **2018**, *57*, 4205–4221.
(18) Vasdev, R. A. S.; Gaudin, L. F.; Preston, D.; Jogy, J. P.; Giles, G. I.; Crowley, J. D. Anticancer Activity and Cisplatin Binding Ability of Bis-Quinoline and Bis-Isochuinoline Derived $[Pd_2L_4]^{4+}$ Metallosupramolecular Cages. *Front. Chem*. **2018**, *6*, 563.
(19) Casini, A.; Woods, B.; Wenzel, M. The Promise of Self-Assembled 3D Supramolecular Coordination Complexes for Biomedical Applications. *Inorg. Chem*. **2017**, *56*, 14715–14729.
(20) Kaiser, F.; Schmidt, A.; Heydenreuter, W.; Altmann, P. J.; Casini, A.; Sieber, S. A.; Kühn, F. E. Self-assembled palladium and platinum coordination cages: Photophysical studies and anticancer activity. *Eur. J. Inorg. Chem.* **2016**, 5189–5196.
(21) Schmidt, A.; Hollering, M.; Drees, M.; Casini, A.; Kuhn, F. E. Supramolecular exo-functionalized palladium cages: fluorescent properties and biological activity. *Dalton Trans*. **2016**, *45*, 8556–8565.
(22) Schmidt, A.; Molano, V.; Hollering, M.; Pöthig, A.; Casini, A.; Kühn, F. E. Evaluation of New Palladium Cages as Potential Delivery Systems for the Anticancer Drug Cisplatin. *Chem. Eur. J.* **2016**, *22*, 2253–2256.
(23) McNeill, S. M.; Preston, D.; Lewis, J. E. M.; Robert, A.; Knerr-Rupp, K.; Graham, D. O.; Wright, J. R.; Giles, G. I.; Crowley, J. D. Biologically active $[Pd_2L_4]^{4+}$ quadruply-stranded helicates: stability and cytotoxicity. *Dalton Trans*. **2015**, *44*, 11129–11136.
(24) Lewis, J. E. M.; Gavey, E. L.; Cameron, S. A.; Crowley, J. D. Stimuli-responsive Pd_2L_4 metallosupramolecular cages: towards targeted cisplatin drug delivery. *Chem. Sci*. **2012**, *3*, 778–784.
(25) Datta, S.; Saha, M. L.; Stang, P. J. Hierarchical Assemblies of Supramolecular Coordination Complexes. *Acc. Chem. Res*. **2018**, *51*, 2047–2063.
(26) Bentz, K. C.; Cohen, S. M. Supramolecular Metallopolymers: From Linear Materials to Infinite Networks. *Angew. Chem. Int. Ed.* **2018**, *57*, 14992–15001.
(27) Gu, Y.; Alt, E. A.; Wang, H.; Li, X.; Willard, A. P.; Johnson, J. A. Photoswitching topology in polymer networks with metal–organic cages as crosslinks. *Nature* **2018**, *560*, 65–69.
(28) Wang, Y.; Gu, Y.; Keeler, E. G.; Park, J. V.; Griffin, R. G.; Johnson, J. A. Star PolyMOCs with Diverse Structures, Dynamics, and Functions by Three-Component Assembly. *Angew. Chem. Int. Ed*. **2017**, *56*, 188–192.
(29) Zhukhovitskiy, A. V.; Zhao, J.; Zhong, M.; Keeler, E. G.; Alt, E. A.; Teichen, P.; Griffin, R. G.; Hore, M. J. A.; Willard, A. P.; Johnson, J. A. Polymer Structure Dependent Hierarchy in PolyMOC Gels. *Macromolecules* **2016**, *49*, 6896–6902.
(30) Zhukhovitskiy, A. V.; Zhong, M.; Keeler, E. G.; Michaelis, V. K.; Sun, J. E. P.; Hore, M. J. A.; Pochan, D. J.; Griffin, R. G.; Willard, A. P.; Johnson, J. A. Highly branched and loop-rich gels via formation of metal–organic cages linked by polymers. *Nature Chemistry* **2015**, *8*, 33–41.
(31) Bardhan, D.; Chand, D. K. Palladium(II)-Based Self-Assembled Heteroleptic Coordination Architectures: A Growing Family. *Chem. Eur. J*. **2019**, *25*, 12241–12269.
(32) Pullen, S.; Clever, G. Mixed-Ligand Metal-Organic Frameworks and Heteroleptic Coordination Cages as Multifunctional Scaffolds–A Comparison. *Acc. Chem. Res*. **2018**, *51*, 3052–3064.
(33) Bloch, W. M.; Clever, G. H. Integrative self-sorting of coordination cages based on 'naked' metal ions. *Chem. Commun*. **2017**, *53*, 8506–8516.
(34) Holloway, L. R.; Bogie, P. M.; Hooley, R. J. Controlled self-sorting in self-assembled cage complexes. *Dalton Trans.* **2017**, *46*, 14719–14723.
(35) Zhu, R.; Bloch, W. M.; Holstein, J. J.; Mandal, S.; Schäfer, L. V.; Clever, G. H. Donor-Site-Directed Rational Assembly of Heteroleptic cis-$[Pd_2L_2L'_2]$ Coordination Cages from Picolyl Ligands. *Chem. Eur. J.* **2018**, *24*, 12976–12982.

(36) Bloch, W. M.; Holstein, J. J.; Hiller, W.; Clever, G. H. Morphological Control of Heteroleptic cis- and trans-$Pd_2L_2L'_2$ Cages. *Angew. Chem. Int. Ed.* **2017**, *56*, 8285–8289.
(37) Preston, D.; Barnsley, J. E.; Gordon, K. C.; Crowley, J. D. Controlled Formation of Heteroleptic $[Pd_2(L_a)_2(L_b)_2]^{4+}$ Cages. *J. Am. Chem. Soc*. **2016**, *138*, 10578–10585.
(38) Bloch, W. M.; Abe, Y.; Holstein, J. J.; Wandtke, C. M.; Dittrich, B.; Clever, G. H. Geometric Complementarity in Assembly and Guest Recognition of a Bent Heteroleptic cis-$[Pd_2L^A_2L^B_2]$ Coordination Cage. *J. Am. Chem. Soc.* **2016**, *138*, 13750–13755.
(39) Yamashina, M.; Yuki, T.; Sei, Y.; Akita, M.; Yoshizawa, M. Anisotropic Expansion of an M_2L_4 Coordination Capsule: Host Capability and Frame Rearrangement. *Chem. Eur. J.* **2015**, *21*, 4200–4204.
(40) Johnson, A- M.; Hooley, R. J. Steric Effects Control Self-Sorting in Self-Assembled Clusters. *Inorg. Chem.* **2011**, *50*, 4671–4673.
(41) Prusty, S.; Yazaki, K.; Yoshizawa, M.; Chand, D. K. A Truncated Molecular Star. *Chem. Eur. J.* **2017**, *23*, 12456–12461.
(42) Howlander, P.; Das, P.; Zangrando, E.; Mukherjee, P. S. Urea-Functionalized Self-Assembled Molecular Prism for Heterogeneous Cataylsis in Water. *J. Am. Chem. Soc.* **2016**, *138*, 1668–1676.
(43) Sun, Q.-F.; Sato, S.; Fujita, M. An $M_{12}(L^1)_{12}(L^2)_{12}$ Cantellated Tetrahedron: A Case Study on Mixed-Ligand Self-Assembly. *Angew. Chem. Int. Ed.* **2014**, *53*, 13510–13513.
(44) Fujita, D.; Suzuki, K.; Sato, S.; Yagi-Utsumi, M.; Yamaguchi, Y.; Mizuni, N.; Kumasaka, T.; Takata, M.; Noda, M.; Uchiyama, S.; Kato, K.; Fujita, M. Protein encapsulation within synthetic molecular hosts. *Nat. Commun*. **2012**, *3*, 1093.
(45) For $PdnL_xL'_y$-type assemblies with $n > 2$ and a non-specific incorporation of two bis-monodentate ligands, see refs. 30 and 46–49:
(46) Frank, M.; Ahrens, J.; Bejenke, I.; Krick, M.; Schwarzer, D.; Clever, G. H. Light-Induced Charge Separation in Densely Packed Donor-Acceptor Coordination Cages. *J. Am. Chem. Soc.* **2016**, *138*, 8279–8287.
(47) Jansze, S. M.; Cecot, G.; Wise, M. D.; Zhurov, K. O.; Ronson, T. K.; Castilla, A. M.; Finelli, A.; Pattison, P.; Solari, E.; Scopelliti, R.; Zelinskii, G. E.; Vologzhanina, A. V.; Voloshin, Y. Z.; Nitschke, J. R.; Severin, K., Ligand Aspect Ratio as a Decisive Factor for the Self-Assembly of Coordination Cages. *J. Am. Chem. Soc*. **2016**, *138*, 2046–2054.
(48) Gramage-Doria, R.; Hessels, J.; Leenders, S. H. A. M.; Tröppner, O.; Dürr, M.; Ivanović-Burmazović, Reek, J. N. H. Gold(I) Catalysis at Extreme Concentrations Inside Self-Assembled Nanopsheres. *Angew. Chem. Int. Ed.* **2014**, *53*, 13380–13384.
(49) Frank, M.; Krause, L.; Herbst-Irmer, R.; Stalke, D.; Clever, G. H. Narcissistic self-sorting vs. static ligand shuffling within a series of phenothiazine-based coordination cages. *Dalton Trans*. **2014**, *43*, 4587–4592.
(50) For heteroleptic Pd assemblies with ligand:Pd ratios other than 2, see refs. 51 and 52.
(51) Wu, K.; Zhang, B.; Drechsler, C.; Holstein, J. J.; Clever, G. H. Backbone-Bridging Promotes Diversity in Heteroleptic Cages, *Angew. Chem. Int. Ed.* **2020**, DOI: 10.1002/anie.202012425.
(52) Samantray, S.; Krishnaswamy, S.; Chand, D. K. Self-Assembled Conjoined-Cages. *Nat. Commun*. **2020**, *11*, 880.
(53) Lehn, J.-M. Dynamic Combinatorial Chemistry and Virtual Combinatorial Libraries. *Chem. Eur. J.* **1999**, *5*, 2455–2463.
(54) Huc, I.; Lehn, J.-M. Virtual combinatorial libraries: Dynamic generation of molecular and supramolecular diversity by self-assembly. *Proc. Natl. Acad. Sci.* **1997**, *94*, 2106–2110.
(55) Hasenknopf, B.; Lehn, J.-M.; Boumediene, N.; Dupont-Gervais, A.; Van Dorsselaer, A.; Kneisel, B.; Fenske, D. Self-Assembly of Tetra- and Hexanuclear Circular Helicates. *J. Am. Chem. Soc*. **1997**, *119*, 10956–10962.
(56) Hasenknopf, B.; Lehn, J.-M.; Kneisel, B. O.; Baum, G.; Fenske, D. Self-Assembly of a Circular Double Helicate. *Angew. Chem. Int. Ed. Engl.* **1996**, *35*, 1838–1840.
(57) Severin, K. The Advantage of being Virtual – Target Induced Adaptation and Selection in Dynamic Combinatorial Libraries. *Chem. Eur. J.* **2004**, *10*, 2565–2580.
(58) Grote, Z.; Scopelliti, R.; Severin, K. Adaptive Behavior of Dynamic Combinatorial Libraries Generated by Assembly of Different Building Blocks. *Angew. Chem. Int. Ed.* **2003**, *42*, 3821–3825.
(59) Chand, D. K.; Biradha, K.; Kawano, M.; Sakamoto, S.; Yamaguchi, K.; Fujita, M. Dynamic Self-Assembly of an M_3L_6 Molecular Triangle and an M_4L_8 Tetrahedron from Naked Pd^{II} Ions and Bis(3-pyridyl)-Substituted Arenes. *Chem. Asian J.* **2006**, *1*, 82–90.
(60) Zhu, R.; Lübben, J.; Dittrich, B.; Clever, G. H. Stepwise Halide-Triggered Double and Triple Catenation of Self-Assembled Coordination Cages. *Angew. Chem. Int. Ed*. **2015**, *54*, 2796–2800.
(61) Sahoo, H. S.; Chand, D. K. Conformation of N,N′-bis(3-pyridylformyl)piperazine and spontaneous formation of a saturated quadruple stranded metallohelicate. *Dalton Trans*. **2010**, *39*, 7223–7225.
(62) Liao, P.; Langloss, B. W.; Johnson, A. M.; Knudsen, E. R.; Tham, F. S.; Julian, R. R.; Hooley, R. J. Two-component control of guest binding in a self-assembled cage molecule. *Chem. Commun.* **2010**, *46*, 4932–4934.
(63) Tominaga, M.; Suzuki, K.; Kawano, M.; Kusukawa, T.; Ozeki, T.; Sakamoto, S.; Yamaguchi, K.; Fujita, M. Finite, Spherical Coordination Networks That Self-Organize from 36 Small Components. *Angew. Chem. Int. Ed*. **2004**, *43*, 5621–5625.
(64) Löffler, S.; Lübben, J.; Krause, L.; Stalke, D.; Dittrich, B.; Clever, G. H. Triggered Exchange of Anionic for Neutral Guests inside a Cationic Coordination Cage. *J. Am. Chem. Soc*. **2015**, *137*, 1060–1063.
(65) This mixture provides good solubility for a range of $[Pd_nL_{2n}]X_n$ complexes.
(66) We have also examined the formation of $[Pd_6(\mathbf{L1})_6(\mathbf{L5})_6](BF_4)_{12}$ starting from $[Pd_4(\mathbf{L1})_8](BF_4)_8$ (3 equiv) and $[Pd_{12}(\mathbf{L5})_{24}](BF_4)_{24}$ (1 equiv). A rearrangement into the heteroleptic cage was observed, but the reaction was not complete after 85 days. For details, see the SI.
(67) Jansze, S. M.; Severin, K. Palladium-Based Metal-Ligand Assemblies: The Contrasting Behavior upon Addition of Pyridine and Acid. *J. Am. Chem. Soc.* **2019**, *141*, 815–819.
(68) Jansze, S. M.; Severin, K. Clathrochelate Metalloligands in Supramolecular Chemistry and Materials Science. *Acc. Chem. Res.* **2018**, *51*, 2139–2147.
(69) Wise, M. D.; Holstein, J. J.; Pattison, P.; Besnard, C.; Solari, E.; Scopelliti, R.; Bricogne, G.; Severin, K. Large, heterometallic coordination cages based on ditopic metallo-ligands with 3-pyridyl donor groups. *Chem. Sci*. **2015**, *6*, 1004–1010.
(70) Jansze, S. M.; Ortiz, O.; Fadei Tirani, F.; Scopelliti, R.; Menin, L.; Severin, K. Inflating Face-Capped Pd_6L_8 Coordination Cages. *Chem. Commun.* **2018**, *54*, 9529–9532.
(71) Jansze, S. M.; Wise, M. D.; Vologzhanina, A. V.; Scopelliti, R.; Severin, K. $Pd^{II}_2L_4$-type coordination cages up to three nanometers in size. *Chem. Sci*. **2017**, *8*, 1901–1908.
(72) Wise, M. D.; Ruggi, A.; Pascu, M.; Scopelliti, R.; Severin, K. Clathrochelate-based bipyridyl ligands of nanoscale dimensions: easy-to-access building blocks for supramolecular chemistry. *Chem. Sci*. **2013**, *4*, 1658–1662.

Graphic for TOC